

Design optimization of magnetorheological damper geometry using response surface method for achieving maximum yield stress[†]

A. J. D. Nanthakumar^{1,*} and J. Jancirani²

¹Department of Automobile Engineering, SRM Institute of Science and Technology, Kattankulathur 603 203, India

²Department of Production Technology, Anna University, M.I.T. Campus, Chromepet, Chennai 600 044, India

(Manuscript Received August 19, 2018; Revised May 7, 2019; Accepted June 19, 2019)

Abstract

Field controllable magnetorheological (MR) damper has gained prominence as a suitable vibration control device for a wide variety of applications as they offer the combined advantages of high-performance metrics of a fully active vibration control system with the cost metrics of a passive vibration control system. The functional quantity that influences the damping performance of a magnetorheological damper is the yield stress of the magnetorheological fluid across the fluid flow gap when the magnetic field is applied. To achieve maximum damping output from the magnetorheological damper, the geometry of the damper piston needs to be optimized. The main geometrical design parameters of the damper piston are the pole width, magnetorheological fluid flow gap, distance between piston rod and coil and the outer pole thickness. The optimization of the damper geometry is carried over with magnetic field strength and yield stress as response variables in two different iterations. A quadratic polynomial function is considered for both the response variables. The yield stress response variable is found to exhibit a more accurate following through the regression equation and it is selected as the response variable of choice. The individual effect of each of the design variable and the interaction effect of the design variables over the yield stress response variable is studied in this research paper. The optimal values of the piston geometry could be used to fabricate a magnetorheological damper prototype in future study.

Keywords: Damper design; Design optimization; Magnetorheological damper; Response surface method; Saturation magnetization; Yield stress

1. Introduction

Magnetorheological effect (MRE) has enabled the engineers for direct electric signal control of the flow and the electric and magnetic characteristics of a fluid medium, which, in its turn, provides new processes and equipments [1]. Magnetorheological fluids (MRF) exhibit yield stress which is limited due to the magnetic saturation occurring in the magnetic circuit. A typical step wise design procedure was suggested involving the number of turns of the coil, path length for electromagnetic flux flow and area ratios [2]. When magnetic suspensions consisting of magnetite particles of dimensions of the order of microns are subjected to a magnetic field, the magnetic particles align themselves in the direction of the field resulting in a fiber structure with the fiber axis aligned along the magnetic field direction. This results in the onset of yield stress which is to be overcome for fluid flow [3]. The maximum value of the stress that can be applied along magnetorheological fluid flow is the yield stress for the fluid. Yield

stress is a function of the magnetic field strength with the relation approximately obeying Bingham's law [4]. The yield stress of the magnetorheological fluids depends on the average particle size of carbonyl iron particles wherein, magnetorheological fluids with finer particles result in lower yield stress values due to smaller magnetization [5]. MR fluid behavior can be assumed to be of viscoelastic behavior with a magnetic field dependent yield stress. Yield stress of MR fluid can be enhanced by magnetic flux effect, weight percentage of suspensions [6]. Shear yield stress of the magnetorheological fluids has a direct ratio to the magnetic saturation intensity [7]. Under combined squeeze and valve modes of operation, the mechanical force property of MR fluid increases linearly with piston velocity [8]. The behavior of MR fluids depends upon the angle of application of external magnetic field with a difference in the magnitude of shear stresses measured for the MR fluid [9]. The yield stress and shear viscosity of MR fluids depend upon the weight percentage of added carbonyl iron particles, weight percentage of additive particles and magnetic field strength [10].

*Corresponding author. Tel.: +91 7810032033

E-mail address: ajd.nanthakumar@gmail.com

[†]Recommended by Associate Editor Jaewook Lee

© KSME & Springer 2019

2. Magnetorheological (MR) devices

2.1 Magnetorheological fluids (MRF)

Magnetorheological fluids were discovered by Jacob Rabinow through experiments conducted at the US National Bureau of Standards [11]. They consist of magnetically polarizable particles dispersed in a non-polar carrier fluid. Usually iron particles in the size of the order of microns obtained from decomposition of iron pentacarbonyl are utilized. The carrier fluids should also possess good thermal stability so that their rheological behavior does not vary with temperature. Usually petroleum-based oils, silicone, mineral oils, polyesters, polyethers, water, synthetic hydrocarbon oils are generally used as carrier fluids. In addition, additives are added as stabilizers and surfactants. They include xantham gum, stearates, silica gel and carboxylic acids. These additives act as thixotropic agents and control sedimentation of particles in the suspension matrix. However, many of the MR fluids exhibit shear thinning nature due to the inclusion of particles and microstructural changes of particles in shear conditions. MR dampers work under flow mode of operation [12].

2.2 Magnetorheological damper applications

Magnetorheological fluid devices which had been developed in the research labs a couple of decades ago have evolved for commercial production [13] due to advance-melts in material science. Magnetorheological devices are classified as fixed pole devices and moveable pole devices. Magnetorheological damper stands as an example for fixed pole device. Magnetorheological dampers have been found utilization in seat suspension systems of heavy-duty vehicles [14] with an innovative rotary design with distinct advantages of usage reduction of the magnetorheological fluid combined with low sealing requirements and correspondingly lower cost. Due to inherent advantages of high dynamic range and low power requirements, MR dampers have been utilized in vibration mitigation of civil structures including earthquake resistant structures [15]. MR dampers have also been employed in smart prosthetic knees based on the kinetic characteristics of the human knees [16] wherein the total energy consumption for the MR damper is minimized. MR dampers have also been deployed as secondary suspension systems in railway suspension systems [17] wherein the large amplitude vibrations of the rail car body can be reduced. MR dampers have also been proposed for controlling the cable vibration of cable stay bridges. With an appropriate semi active control algorithm [18], the effectiveness of a MR damper for controlling the cable vibration have been assessed. An adaptive MR damper for landing gears of light weight helicopters have been developed [19]. MR dampers have found applications in off road vehicles and military combat vehicles [20] which require a heavy damping force and fast response with a heavy payload requirement. MR damper in combination with a safety passive damper can be utilized as a semi active suspension system in

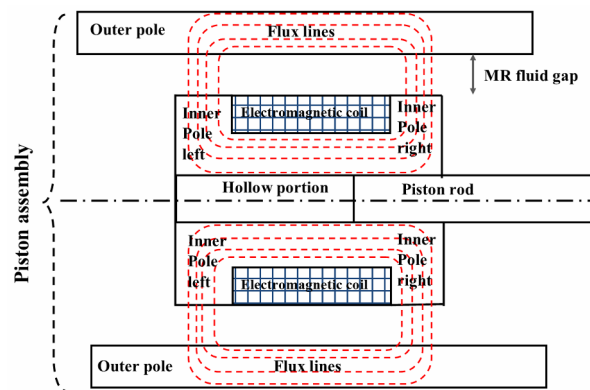


Fig. 1. Flow of magnetic flux lines in a MR damper.

military vehicles with substantial improvement in ride quality and road holding characteristics. The model for the magnetorheological damper is derived by forming the expression for pressure drop developed in the magnetorheological fluid flow due to viscosity and the yield stress.

The MR damper is functionally similar to a conventional damper with few unique differences in the constructional features. Most of the MR dampers follow the conventional damper including piston cylinder assembly in construction with changes in the orifice geometry and provision for electromagnetic coil installation [21]. Conventional dampers have a number of circular orifices for damping functionality whereas MR dampers include an annular orifice. Annular orifice aids in achieving maximum utilization of magnetic flux passing through the MR fluid. The outer cylinder of the assembly serves as a flux return path. Fig. 1 shows the flow of magnetic flux lines in a mono coil MR damper analyzed in this paper. Double coil designs [22] and even tri coil designs are also in practice. When current is passed through the coil, magnetic flux is generated. It passes from the inner pole, jumps to the outer pole across the MR fluid flow gap.

3. Magnetorheological damper design

3.1 Basic geometry

MR fluid gap is generally kept in the range of 0.5 mm to 2 mm beyond which the magnetorheological effect cannot be completely harnessed. The magnetic flux traverses across the outer pole and reaches the inner pole through the magnetorheological fluid gap thus forming a closed magnetic loop. Premalatha et al. [23] prepared magnetorheological fluids and analyzed their flow behavior with respect to internal structure and rheological properties. The viscoelastic properties of the magnetorheological fluid were measured by steady state and oscillatory experiments.

3.2 Geometrical parameters

The geometrical parameters of a magnetorheological damper are classified into two types:

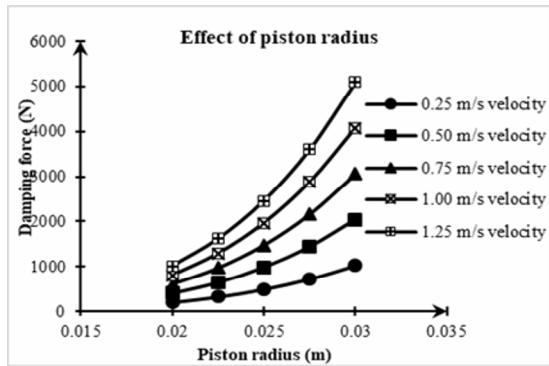


Fig. 2. Piston radius vs damping force.

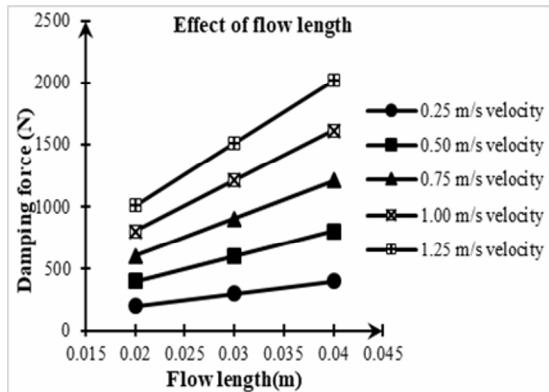


Fig. 3. Flow length vs damping force.

1. Geometrical parameters for the OFF state.
2. Geometrical parameters for the ON state.

OFF state represents the magnetorheological damper operating under no current conditions. ON state represents the damper operating under current applied conditions. The OFF state geometrical parameters are obtained from the flow equation of a fluid across an annular orifice. The basic expression for pressure difference due to viscous effects in an annular orifice involves two parameters, the radius of the piston and the overall flow length through which the magnetorheological fluid is made to flow through. The base damping capacity of the magnetorheological damper is decided by the selection of the OFF-state parameters. Fig. 2 shows the variation of base damping force capacity of a magnetorheological damper with the increase in radius of the piston. The plot is drawn for different values of piston velocities when the damper is subjected to vibration input. The radius of the piston is the primary design variable with which the OFF-state damping capacity of the magnetorheological damper can be controlled. Overall flow length of the magnetorheological fluid inside the damper piston also influences the OFF-state damping capacity. Fig. 3 shows the variation of base damping force capacity of the magnetorheological damper with the increase in flow length of the MR fluid in the piston. In the present research work, the radius of the piston is taken as 0.02 m and the overall flow length as 0.02 m.

The ON state condition represents the generation and flow

Table 1. ON state geometrical parameters in Fig. 4.

ON state geometrical parameter with notation	Lower bound value (mm)	Upper bound value (mm)
Distance between piston rod and coil (1-cph)	3	7
Pole length (2- pw)	5	15
MR fluid flow gap (3-gap)	0.5	1.5
Outer pole thickness (4-opt)	4	8

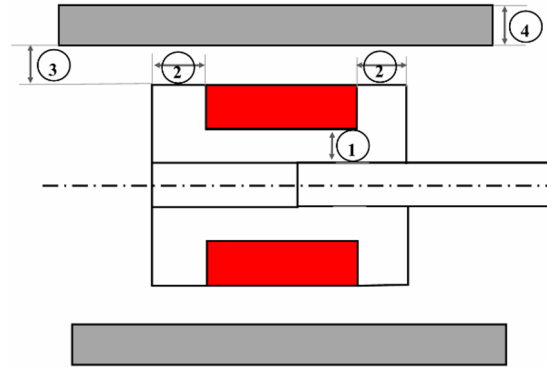


Fig. 4. ON state geometrical parameters.

of magnetic flux through the piston working domain due to flow of current in the electromagnetic coil. The geometric parameters that influence the path of the magnetic flux flow are the ON state parameters. Fig. 4 shows the ON state geometrical parameters. The upper and lower bounds of the ON state geometrical parameters are given in Table 1. Apart from the geometrical parameters shown above, there are electromagnetic properties of the working domain. They include the permeability property of the materials used in the construction of the damper, number of turns in the electromagnetic coil and the magnitude of current flowing through the coil.

3.3 Yield stress

When a magnetic field is applied across the magnetorheological fluids, the ferrous particles present in the fluid align themselves along the direction of the field to form chain structures or clusters. The effective result of the chain formation is the increase in the yield stress of the magnetorheological fluid. When the magnetic field is removed, the chain formation is collapsed and the magnetorheological fluid returns to its original state within a few microseconds making the phase transition process reversible with a response time of few microseconds. Tang et al. [24] discussed that the yield stress of the magnetorheological fluid depended on the solid structures induced due to the application of the magnetic field. Thick columnar structures are needed to improve the yield stress instead of a single/few columnar structures. The yield stress can further be increased by compressing the magnetorheological fluid during the application of the magnetic field. The dependence of yield stress on magnetic field strength can be

divided into two regimes [25]. At low magnetic field strengths, the yield stress is proportional the magnetic field strength squared. At magnetic field strengths near the saturation levels, the yield stress varies sub quadratically with the magnetic field strength. Shah and Choi [26] investigated the field dependent rheological properties for magnetorheological fluids. It was found that magnetorheological particles consisting large sized particles exhibit high yield stress and strong chain structure formation under the application of an external magnetic field. The yield stress of the magnetorheological fluid is dependent on the externally applied magnetic field strength with deviations for particle size, volume ratio and permeability of particle material.

When magnetorheological fluids are subjected to an externally applied magnetic field, a state transition occurs in the fluid domain wherein the fluid changes its phase to a semi solid condition. The state transition of the magnetorheological fluid after the application of the magnetic field can be depicted by the increase in yield stress as a function of the magnetic field strength. The constitutive model for shear yield stress [27] can be expressed as a state transition equation consisting of an expression that relates the yield stress (τ_y) with the fluid composition, applied stimulus and particle volume fraction which is given by Eq. (1).

$$\tau_y = \left[\left[1 + \left(\frac{H}{\alpha\phi^2 + \beta\phi + \chi} \right)^{-B_{MRF}} \right]^{-1} \times \left[\frac{4}{5^{3/2}} \xi(3) \mu_0 M_s^2 \right] \right] \quad (1)$$

The values of the parameters in Eq. (1) are given in Table 2. H represents the magnetic field strength in the magnetorheological fluid domain given in A/m, μ_0 is the permeability constant of free space or vacuum, α , β , χ , B_{MRF} , $\xi(3)$ and M_s are material constants determined from experimental data [27] for the magnetorheological fluids MRF-122EG, MRF-132DG and MRF-140CG supplied by Lord Corporation. The present research work is based on the magnetorheological fluid MRF-122EG. The OFF-state viscosity of MRF-122EG is 0.042 Pa-s and the OFF-state density is 2280 kg/m³ with operating temperature conditions of -40 °C to 130 °C. Thus, MRF-122EG is well suited for dampers fitted in most of the vibration control systems. The calculation of yield stress necessitates the determination of the magnetic field strength in the magnetorheological fluid domain wherein the magnetic flux lines pass through which is the region between inner poles and the outer pole.

4. Determination of magnetic field strength (H)

4.1 Magnetostatic analysis

The magnetic field strength can be determined by performing a magnetostatic analysis of the magnetorheological

Table 2. Parameters of the yield stress Eq. (1) [27].

MR fluid / parameter	MRF - 122EG	MRF - 132DG	MRF - 140CG
α	1547.2		
β	844		
χ	-30.544		
Φ	0.22	0.32	0.40
B_{MRF}	2.41		
$\xi(3)$	1.202		
M_s	831.23 kA/m		

damper domain through which the generated magnetic flux passes through as depicted in Fig. 1. The piston assembly is geometrically similar about the piston axis. Thus, an axisymmetric analysis of the geometry is sufficient to solve the problem instead of analyzing the complete geometry. Finite element analysis is employed for the magnetostatic analysis of the working domain. Comsol multiphysics software is utilized for the purpose. The software is capable of solving the Maxwell's equation in the computational domain and present the magnetic field strength at the point of interest.

4.2 Finite element analysis

Fig. 5 depicts the axisymmetric model constructed in the evaluation version of Comsol multiphysics software. The dimensions of the axisymmetric model are the lower bound values of the geo-metrical parameters as given in Table 1. AC/DC interface is used for solving the problem as the magnetic field quantities have to be determined. Then the magnetic fields (mf) module is selected with a stationary study procedure as the problem is solved as a magnetostatic problem.

The whole axisymmetric model is included as the domain for the magnetic fields study. The piston rod is made of stainless steel of non-ferromagnetic type with a relative permeability of 1 to ensure that magnetic field is not allowed to pass inside the piston rod so that flux leakage is reduced.

The coil portion is attributed with copper material representing the material used in coil windings. The outer poles and inner poles are attributed with a material of high permeability value as well as economical to be used in the prototype fabrication. Hence, AISI 1040 steel with a high relative permeability of 2000 is used for the pole domain. The magnetorheological fluid domain is attributed with the fluid properties of MRF-122EG supplied by Lord Corporation, USA whose relative permeability is around 6. The hollow portion of the axisymmetric model is attributed with the properties of air with a relative permeability of 1. The domain is meshed with a triangular mesh with 159 edge elements and 22 vertex elements. The total number of elements is 794 with a minimum element size of 0.0075 mm and maximum element size of 1.68 mm. A minimum element quality of 0.7061 and an average element quality of 0.9324 is maintained for meshing the domain.

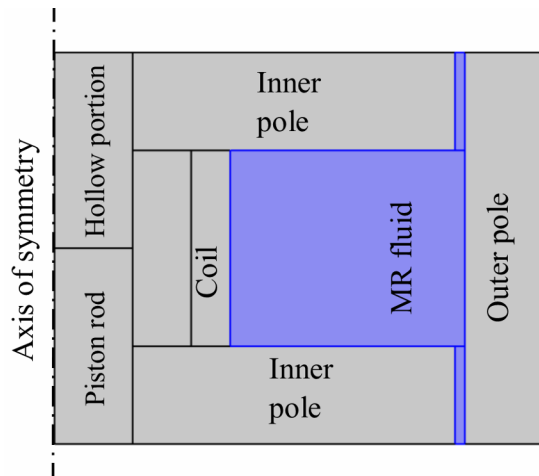


Fig. 5. Axisymmetric model.

The axisymmetric condition is implemented by selecting the axis line of piston as the symmetry axis. The outer boundaries of the domain are attributed with magnetic insulation condition assuming the magnetic flux leakage to be zero. The coil portion is attributed with the coil boundary condition of the magnetic fields module with SWG 35 wire dimensions. The ampere law domain is attributed to all the domains excluding the coil domain. The number of turns of the coil is 300 with a current flow of 0.25 ampere.

The finite element problem was solved in a computing machine with AMD 64-bit processor possessing quad cores with a maximum processor frequency of 3.5 GHz. The RAM capacity of the computing machine is 8 gigabytes with a discrete graphics memory of 2048 megabytes. Comsol multiphysics solves the finite element problem using the MUMPS solver with a tolerance factor 1 of and a residual factor of 1000. Comsol multiphysics suite is capable of plotting the variation of magnetic field strength (H) and the flux flow streamlines inside the problem domain.

Fig. 6 depicts the magnetic field strength (H) inside the domain in two dimensions whereas Fig. 7 depicts the magnetic field strength (H) inside the domain in three dimensions. An initial study is conducted to determine the approximate saturation levels for the electromagnetic domain. For this purpose, simulation studies are carried out using Comsol multiphysics software by varying the input given to the coil. This can be achieved by varying the number of coils and the magnitude of current flowing through the coil. The yield stress is plotted against the current magnitude as shown in Fig. 8.

It is understood from Fig. 8 that the saturation levels of the electromagnetic circuit are approximately achieved around 1 ampere of current. Moreover, complete saturation occurs before 1.5 amperes of current. It indicates that the yield stress does not increase, and it saturates when the current value crosses 1 ampere. Hence the damping force due to magnetorheological effect cannot be improved beyond a current value of around 1 ampere. The damping force generated for a specified current value can also be determined [28]. The numerical

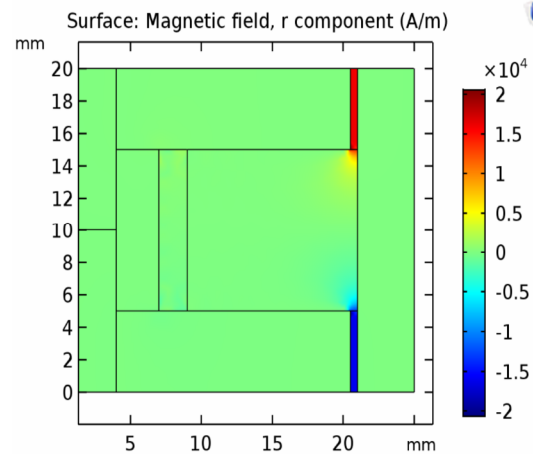


Fig. 6. Variation of magnetic field strength in 2D.

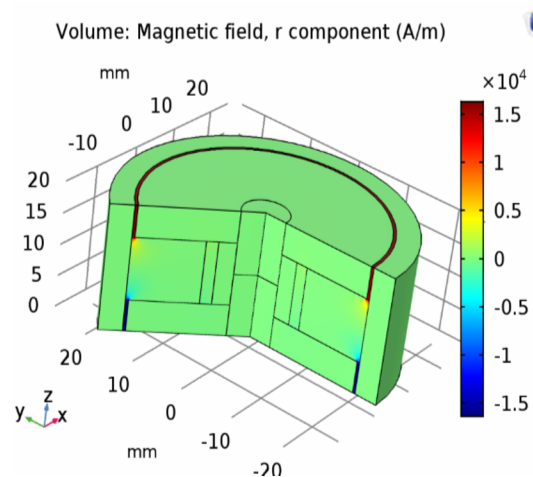


Fig. 7. Variation of magnetic field strength in 3D.

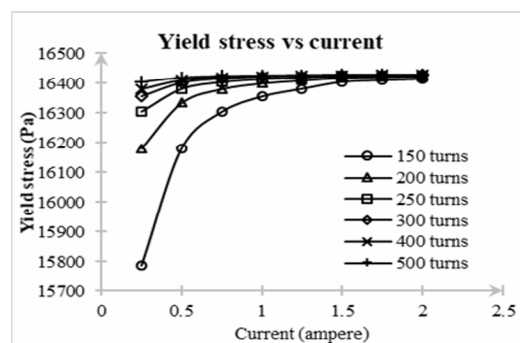


Fig. 8. Determination of saturation level of the circuit.

output obtained from the finite element analysis are mapped with response surface method for performing an optimization study [29].

5. Optimization of MR damper design

Hadadian et al. [30] developed response surface functions

for the magnetic field intensity across the active length of the magnetorheological fluid flow gap. Ferdaus et al. [31] simulated the MR damper through finite element analysis for different configurations of piston, fluid gap, air gap and damper housing. Parlak [32] carried out a design optimization method that had magnetic flux density and damper force as the objective functions. The magnetostatic analysis and CFD analysis was executed through ANSYS modules. Most of the researchers [30-32] who carried out design optimization of MR dampers laid emphasis on optimizing the MR damper geometry for maximum magnetic field intensity and flux density. In this research paper, the magnetorheological piston damper geometry is optimized for maximizing the response variables of magnetic field strength (H) and yield stress. For both the cases, a quadratic regression equation is considered.

5.1 Design of experiments (DoE)

The objective is to find a response function that can model approximately the response variables of magnetic field strength and yield stress across the entire design region. In such design problems, the design optimization of the magnetorheological device is usually conducted inside the finite element analysis software platform which is employed for magnetic analysis. This leads to increase in computational resources and time as each optimization run requires individual analysis of the model in the analysis software. In many of the situations, the optimization is conducted using low order optimization methods available in the analysis software. As an alternate methodology, the finite element analysis is performed at few well-chosen design points that was selected using design of experiments (DoE) technique [33]. The analytical polynomial function is then fitted to the results of the design problem. The design of experiments methodology ensures that all the factors influencing the final response and their interactions are investigated systematically.

5.2 Regression equation

The most extensive employment of response surface method (RSM) technique are for situations where several input variables (design variables) influence the performance metric (response variable) of any process. RSM involves the exploration of the space of design variables, statistical modeling for development of an approximate relationship between the input variable and the response variable and optimization methods to find the values of the design variables that lead to the desired value of the response variable.

The best treatment (optimal sets of design variables) for the design problem obtained using design of experiments and fed to the finite element analysis software gives the magnetic field strength (H) values. RSM is used to map analytical function for the yield stress derived from magnetic field strength values. RSM involves creation of meta-models for the magnetic field strength derived yield stress. The meta model is constructed

from sample data obtained from either practical experiments or numerical experiments like finite element method. The response function obtained from RSM is smooth and thus can be utilized for gradient based or non-gradient based optimization algorithm.

The statistical technique of regression analysis is employed to obtain the response function. When more than one design variable (predictor variable) is involved, multiple regression models are used. The general formation for the regression analysis is shown in Eq. (2).

$$y = \hat{y}(x_1, x_2, x_3, x_4, \dots) + \varepsilon \quad (2)$$

wherein y represents the accurate response, \hat{y} represents the approximation of y . x_1, x_2, x_3 are the design variables and ε is the error between the accurate response and its approximation. The approximation function should be selected in such a way that the error for all the points in the design space are minimized. Generally, polynomial functions are used as regression models of approximation functions. The polynomial functions are generally in the form of Eq. (3).

$$\hat{y} = \beta_0 + \sum_{i=1}^N \beta_i x_i + \sum_{i=1}^N \beta_{ij} x_i x_j + \sum_{i=1}^N \beta_{ii} x_i^2 + \dots \quad (3)$$

The main objective of regression analysis is to determine the most suitable and unbiased estimator of coefficients β for which the error ε is minimized. For the proposed design, a full factorial design with the four factors (Table 1) is considered. Three levels are included for each factor resulting 81 runs for a full factorial design. The magnetic field strength for each design set is found using Comsol multiphysics software using parametric sweep functionality. To estimate the yield stress values, the magnetic field strength values are substituted in Eq. (1) and the yield stress for the magnetorheological fluid flow is determined. A quadratic polynomial function is considered for both magnetic field strength and yield stress wherein linear terms represent each of the factors, square terms of each of the factors and two-way interaction terms represent the interaction between the parameters. The regression equation of the magnetic field strength response variable is given by Eq. (4).

$$\begin{aligned} H = & 375.7 + 88.3cph - 176.9gap + 5.9opt - 53.17pw \\ & + 5.50cph * cph + 24.5gap * gap + 1.74opt * opt \\ & + 3.269pw * pw - 7.83cph * gap + 6.620cph * opt \\ & - 8.458cph * pw - 1.87gap * opt + 10.11gap * pw \\ & - 3.148opt * pw - 9.77 * gap * pw + 14.56 * opt * pw. \end{aligned} \quad (4)$$

The regression equation of the yield stress response variable is given by Eq. (5).

Table 3. Optimal values of the response variables.

Response variable	Regression equation output	FEA output	Variation
Magnetic field strength (A/m)	1109.5	1374	19.2 %
Yield stress (N/m ²)	16518	16411.6	-0.6 %

Table 4. Values of the design variables for optimal yield stress.

Design variable	cph (mm)	gap (mm)	opt (mm)	pw (mm)
Values for optimal yield stress	5.7475	0.5	4	5

Yield stress =

$$\begin{aligned}
 &14987 + 800.5 * cph - 628 * gap + 181 * opt \\
 &- 325.5 * pw - 78.97 * cph * cph + 30 * gap * gap \\
 &+ 4.49 * opt * opt - 5.30 * pw * pw + 65.6 * cph * gap \\
 &- 40.85 * cph * opt + 47.75 * cph * pw + 32.4 * gap * opt \\
 &- 9.77 * gap * pw + 14.56 * opt * pw .
 \end{aligned}
 \tag{5}$$

The above regression equations are optimized for maximum values. The evaluation version of Minitab software is used for performing the optimization study and finding the maximum values. The maximum values obtained for the yield stress and magnetic field strength response variables from the quadratic regression equations are compared with experimental values (finite element analysis output) in Table 3. It is clearly found that yield stress regression equation is more relevant with the optimization study as the regression analysis output is varying by only -0.6 % with the experimental (FEA) output. Thus, the yield stress is favored for the selection of response variable for optimization with a quadratic regression equation. It is the primary function of a designer to check statistically the accuracy of the quadratic model developed so that the developed model provides an accurate representation of the true response. The main quantity used to check the accuracy of RSM models is the co-efficient of multiple de-termination R² that depicts the variation within the output response. The quadratic function developed has a R² value of 97.83 %. The adjusted R² value is 97.37 % and the predicted R² value for the expression is 96.55 %.

5.3 Plots for yield stress

The end objective is to optimize the response variable - yield stress, which is influenced by design variables representing the geometrical parameters of the magnetic circuit. The advantage of the RSM tool is its capability to analyze the effect of varying design variables individually and in combination over the response variable through graphs and surface areas. In this research paper, the effect of variation of the four design variables (pw, gap, cph and opt) on the response vari-

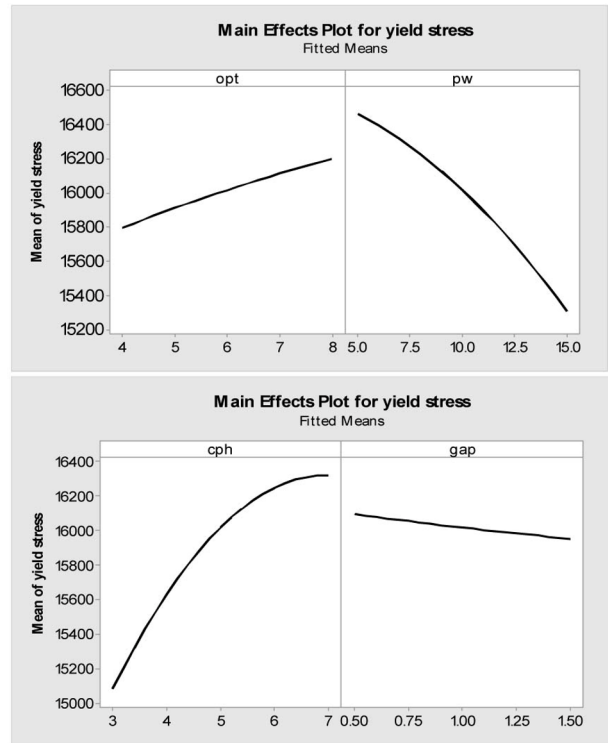


Fig. 9. Main effects of design variables.

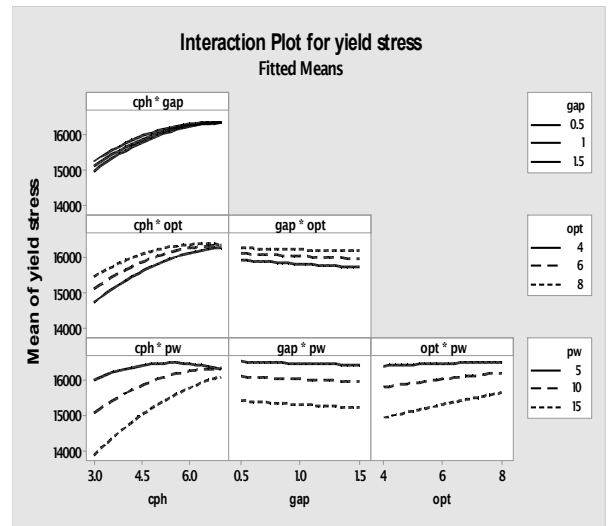


Fig. 10. Interaction effects of design variables.

able (yield stress) is studied. The main effects of the four design variables are shown in the graphs depicted in Fig. 9. The interaction effects for the geometrical parameters are shown in the graphs in Fig. 10.

Figs. 11-16 show the surface plots for the interaction between two design variables taken at a time keeping the other two variables constant. These surface plots represent the variation and distribution pattern in the magnetic field strength induced yield stress of the magnetorheological fluid.

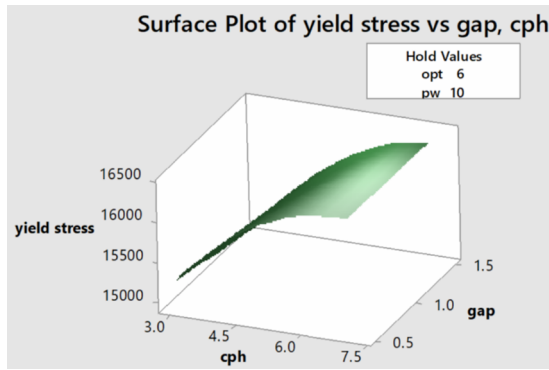


Fig. 11. Surface plot for variations in cph and gap.

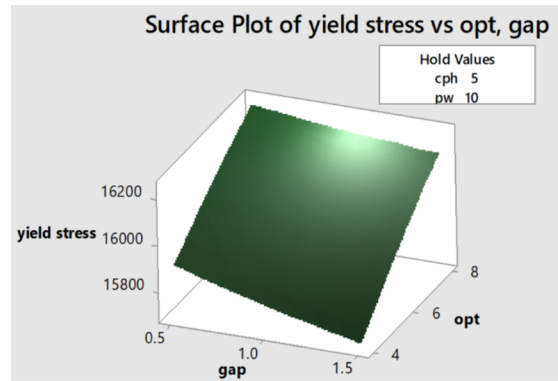


Fig. 14. Surface plot for variations in opt and gap.

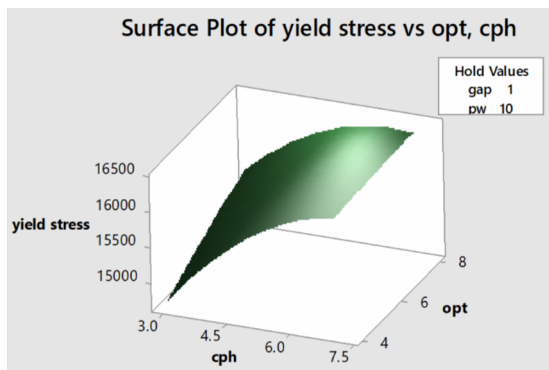


Fig. 12. Surface plot for variations in opt and cph.

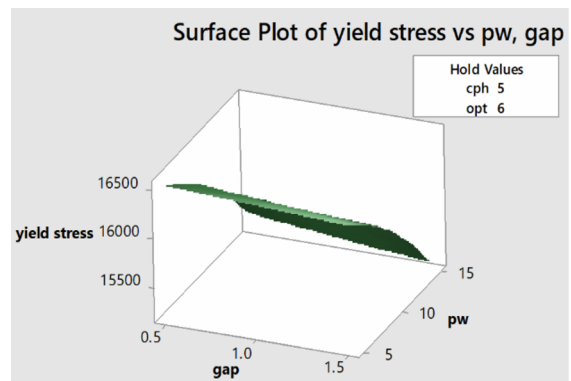


Fig. 15. Surface plot for variations in pw and gap.

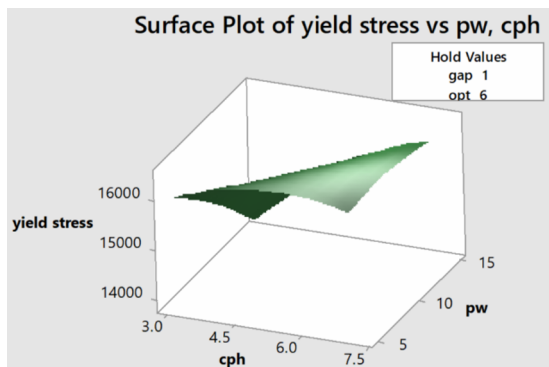


Fig. 13. Surface plot for variations in pw and cph.

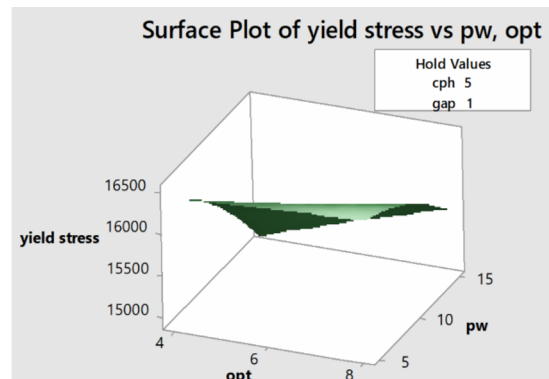


Fig. 16. Surface plot for variations in pw and opt.

5.4 Response optimization

The response of magnetic field strength induced yield stress is optimized for the given geometric boundary conditions of the design variables as listed in Table 1. The optimization is carried for maximizing the yield stress dependent on magnetic field strength at the magnetorheological fluid flow gap. The solution for the optimization problem is given as an yield stress of 16518 N/m² for the magnetic circuit geometrical values of magnetorheological fluid flow gap (gap) of 0.5 mm, outer pole thickness (opt) of 4 mm, pole length (pw) of 5 mm and distance between piston rod and coil (cph) of 5.74747 mm.

6. Results and discussion

In the initial part of the study, the magnetic field strength and yield stress were considered for response optimization. A quadratic regression analysis was carried over and the yield stress was found to be the appropriate response variable for optimization study as given in Table 3. From Fig. 9, it is evident that out of the four magnetic circuit geometric parameters, the pole length (pw) and the distance between piston rod and coil (cph) shows an appreciable variability for magnetic field

strength induced yield stress within the boundary limits. A high variability is necessary for achieving maximum dynamic ratio of the magnetorheological damper which is an essential design requirement. Fig. 10 shows the interaction effects between the design variables. Out of all the interaction effects, the graphs involving distance between piston rod and coil (cph) shows the maximum variability. Moreover, the interaction effects involving distance between piston rod and coil (cph) and pole length (pw) shows the maximum variability for the response function.

Fig. 11 shows the surface plot for the design variables of distance between piston rod and coil (cph) and magnetorheological fluid flow gap (gap). It is evident from the graph that maximum values of magnetic field strength-based yield stress are obtained for higher cph values. The increase in gap did not increase the yield stress considerably. This effect can be attributed to the fact that when the distance between piston rod and coil (cph) is more, the magnetic circuit is capable of passing more amount of flux lines with least reluctance. Fig. 12 shows the surface plot for the design variables of outer pole thickness (opt) and distance between piston rod and coil (cph). It is evident from the graph that magnetic field strength dependent yield stress is maximum when the values of cph and opt both are higher. Fig. 13 shows the surface plot for the design variables of pole length (pw) and distance between piston rod and coil (cph). The graph shows a surface for which the maxima value occurs in the middle of the surface plot approximately along a linear straight-line curve. This indicates the effect that when the distance between piston rod and coil (cph) is lower the pole length (pw) should be correspondingly lower for achieving maximum field strength dependent yield stress. If the pole length is larger, it leads to low magnetic flux density distribution thus resulting in lower magnetorheological effect. On the other side, when the distance between piston rod and coil (cph) is higher, the pole length should be correspondingly higher to accommodate the more amount of magnetic flux lines to pass through. The same effect is seen in the interaction effect graph shown in Fig. 10 wherein the graph between cph*pw shows the magnetic field strength dependent maximum yield stress converges to a small area which can be approximated for a point.

Fig. 14 shows the surface plot for the design variables of outer pole thickness (opt) and magnetorheological fluid flow gap (gap). The surface plot approximately yields to a flat surface with minimum curvature indicating the effects of opt and gap are linear towards the response variable. The maximum value of the response variable, magnetic field strength dependent yield stress occurs at low gap and high opt values. A similar effect is seen in Fig. 10 in which the interaction effects for the design variables of gap*opt are seen as linear curves with minimum variability in the response variable. Fig. 15 shows the surface plot for the design variables of magnetorheological fluid flow gap (gap) and pole length (pw). The maximum of magnetic field strength dependent yield stress is obtained when both the design variables of gap and pw are

minimum. On the other hand, when these design variables are high the response variable becomes lower. This is due to the fact that when the gap and pw are higher, the magnetic flux density is lower resulting in lesser amount of flow of magnetic flux lines leading to a lower yield stress. Fig. 16 shows the surface plot for the design variables of pole length (pw) and outer pole thickness (opt). The magnetic field strength dependent yield stress is maximum when pole length (pw) is minimum. The outer pole thickness (opt) shows a linear relation with the response variable. The same effect is also seen in the interaction plot of opt*pw as shown in Fig. 10.

7. Conclusions

The present research work has identified the design variables for the geometry of a magnetic circuit in a magnetorheological damper. The effect of each of the design variable on the output response of yield stress has been studied. The interaction effects of the design variables have also been studied. An optimization exercise has been carried over after formulating a quadratic expression for the response variable through design of experiments in a full factorial study. The magnetic field strength has been found out using magnetic field module of evaluation version of Comsol multiphysics software and the optimization study has been carried over in evaluation version of Minitab software. The present research work has been carried over for a representative magnetorheological damper. The same design and optimization procedure can be extended for magnetorheological dampers used for applications with varying payloads from prosthetic dampers to large scale dampers used in earth quake resilient structures. The base damping capacity for the magnetorheological dampers can be varied by changing the piston dimensions and length of flow of the magnetorheological fluid inside the piston. The effect of magnetic circuit geometric parameters representing the distance between piston rod and coil (cph) and pole length (pw) are found to be more sensitive in achieving the response of the MR damper.

Nomenclature

<i>cph</i>	: Distance between piston rod and coil
<i>gap</i>	: Magnetorheological fluid flow gap
<i>H</i>	: Magnetic field strength
<i>opt</i>	: Outer pole thickness
<i>pw</i>	: Pole width
x_i	: Design variables in regression analysis
<i>y</i>	: Response variable in regression analysis
\hat{y}	: Approximate value of response variable <i>y</i>
$\alpha, \beta, \chi, B_{MRF}, \zeta(3), M_s$: Material constants for the MR fluid
β_i	: Co-efficients of regression function equation
ε	: Error between accurate response and approximate response of the response variable
μ_0	: Permeability of free space
τ_y	: Yield stress of the MR fluid

References

- [1] V. I. Kordonsky, Z. P. Shulman, S. R. Gorodkin, S. A. Demchuk, I. V. Prokhorov, E. A. Zaltsgendler and B. M. Khusid, Physical properties of magnetizable structure-reversible media, *Journal of Magnetism and Magnetic Materials*, 85 (1-3) (1990) 114-120.
- [2] J. H. Kim, C. W. Lee, B. B. Jung and Y. Park, Design of magneto-rheological fluid based device, *Journal of Mechanical Science and Technology*, 15 (11) (2001) 1517-1523.
- [3] E. Lemaire, G. Bossis and Y. Grasselli, Yield stress and structuration of magnetorheological suspensions, *Journal of Magnetism and Magnetic Materials*, 122 (1-3) (1993) 51-52.
- [4] A. G. Olabi and A. Grunwald, Design and application of magneto-rheological fluid, *Materials and Design*, 28 (10) (2007) 2658-2664.
- [5] S. Genc, P. P. Phule and M. K. Kim, Rheological properties of magnetorheological fluids, *Smart Materials and Structures*, 11 (1) (2002) 140-146.
- [6] C. F. Omidbeygi and S. H. Hashemabadi, Experimental study and CFD simulation of rotational eccentric cylinder in a magnetorheological fluid, *Journal of Magnetism and Magnetic Materials*, 324 (13) (2012) 2062-2069.
- [7] Y. Jin, P. Q. Zhang, X. H. Wang and S. J. Wu, Numeric computation on shear yield stress of magnetorheological fluids, *Journal of China Univ. Sci. Technol.*, 31 (2001) 168-173.
- [8] P. Wang and Z. Wang, Determination of the flow stress of a magnetorheological fluid under three-dimensional stress states by using a combination of extrusion test and FEM simulation, *Journal of Magnetism and Magnetic Materials*, 419 (2016) 255-266.
- [9] E. Dohmen, D. Borin and A. Zubarev, Magnetic field angle dependent hysteresis of a magnetorheological suspension, *Journal of Magnetism and Magnetic Materials*, 443 (2017) 275-280.
- [10] E. Esmailnezhad, H. J. Choi, M. Schaffie, M. Gholizadeh, M. Ranjbar and S. H. Kwon, Rheological analysis of magnetite added carbonyl iron based magnetorheological fluid, *Journal of Magnetism and Magnetic Materials*, 444 (2017) 161-167.
- [11] J. Rabinow, The magnetic fluid clutch, *AIEE Transactions*, 67 (2) (1948) 1308-1315.
- [12] J. D. Carlson and M. R. Jolly, MR fluid, foam and elastomer devices, *Mechatronics*, 10 (4-5) (2000) 555-569.
- [13] J. D. Carlson, D. M. Catanzarite and K. A. St. Clair, Commercial magneto-rheological fluid devices, *International Journal of Modern Physics B*, 10 (23-24) (1996) 2857-2865.
- [14] S. S. Sun, D. H. Ning, J. Yang, H. Du, S. W. Zhang and W. H. Li, A seat suspension with a rotary magnetorheological damper for heavy duty vehicles, *Smart Materials and Structures*, 25 (10) (2016) 105032.
- [15] G. Yang, B. F. Spencer Jr., H.-J. Jung and J. D. Carlson, Dynamic modeling of large-scale magnetorheological damper systems for civil engineering applications, *Journal of Engineering Mechanics*, 130 (9) (2004) 1107-1114.
- [16] F. Gao, Y.-N. Liu and W.-H. Liao, Optimal design of a magnetorheological damper used in smart prosthetic knees, *Smart Materials and Structures*, 26 (3) (2017) 01-09.
- [17] S. K. Sharma and A. Kumar, Ride performance of a high speed rail vehicle using controlled semi active suspension system, *Smart Materials and Structures*, 26 (5) (2017) 055026.
- [18] H. Huang, J. Liu and L. Sun, Full-scale experimental verification on the vibration control of stay cable using optimally tuned MR damper, *Smart Structures and Systems*, 16 (6) (2015) 1003-1021.
- [19] Y.-T. Choi, R. Robinson, W. Hu, M. N. Wereley, S. T. Birchette, O. A. Bolukbasi and J. Woodhouse, Analysis and control of a magnetorheological landing gear system for a helicopter, *Journal of the American Helicopter Society*, 61 (3) (2016) 1-8.
- [20] S. H. Ha, M.-S. Seong and S.-B. Choi, Design and vibration control of military vehicle suspension system using magnetorheological damper and disc spring, *Smart Materials and Structures*, 22 (6) (2013) 01-10.
- [21] S. K. Mangal and A. Kumar, Experimental and numerical studies of magnetorheological (MR) damper, *Chinese Journal of Engineering*, 2014 (2014) 915694: 01-07.
- [22] G. Hu, M. Long, M. Huang and W. Li, Design, analysis, prototyping, and experimental evaluation of an efficient double coil magnetorheological valve, *Advances in Mechanical Engineering*, 6 (2014) 01-09.
- [23] S. E. Premalatha, R. Chokkalingam and M. Mahendran, Magneto mechanical properties of iron based MR fluids, *American Journal of Polymer Science*, 2 (4) (2012) 50-55.
- [24] X. Tang, X. Zhang and R. Tao, Structure-enhanced yield stress of magnetorheological fluids, *Journal of Applied Physics*, 87 (5) (2000) 1107-1114.
- [25] J. de Vicente, D. J. Klingenberg and R. Hidalgo-Alvarez, Magnetorheological fluids: A review, *Soft Matter*, 7 (2011) 3701-3710.
- [26] K. Shah and S.-B. Choi, The field-dependent rheological properties of magnetorheological fluids featuring plate-like iron particles, *Frontiers in Materials*, 1 (2014) 01-21.
- [27] M. I. Varela-Jiménez, J. L. Vargas Luna, J. A. Cortés-Ramírez and G. Song, Constitutive model for shear yield stress of magnetorheological fluid based on the concept of state transition, *Smart Materials and Structures*, 24 (4) (2015) 045039: 1-7.
- [28] J. Jancirani, A. J. D. Nanthakumar and P. Niketh, Optimal current value estimation for an automotive magneto rheological (MR) fluid damper actuation, *Applied Mechanics and Materials*, 812 (2015) 93-101.
- [29] S. Seid, C. Sujatha and S. Sujatha, Optimal design of an MR damper valve for prosthetic knee application, *Journal of Mechanical Science and Technology*, 32 (6) (2018) 2959-2965.
- [30] A. Hadadian, R. Sedaghati and E. Esmailzadeh, Design optimization of magnetorheological fluid valves using response surface method, *Journal of Intelligent Material Sys-*

tems and Structures, 25 (11) (2018) 1352-1371.

- [31] M. M. Ferdous, M. M. Rashid, M. H. Hasan and M. A. Rahman, Optimal design of magneto-rheological damper comparing different configurations by finite element analysis, *Journal of Mechanical Science and Technology*, 28 (9) (2014) 3667-3677.
- [32] Z. Parlak, T. Engin and I. Çallı, Optimal design of MR damper via finite element analyses of fluid dynamic and magnetic field, *Mechatronics*, 22 (6) (2012) 890-903.
- [33] D. C. Montgomery, *Design and Analysis of Experiments*, 5th Edition, John Wiley & Sons Inc. (2008).



J. Jancirani is a Professor in the Department of Production Technology at Anna University, MIT Campus, Chennai, India. Her main research areas include vehicle dynamics, automotive braking systems and CAD.



A. J. D. Nanthakumar is an Assistant Professor in the Department of Automobile Engineering at SRM Institute of Science and Technology, Kattankulathur, India. His main research areas include vehicle dynamics, vibration damping and non-newtonian fluids rheology.